Synthesis, Crystal Structure, and Thermal Decomposition Kinetics of the Ternary Complex $[Sm(5\text{-Cl-2-MOBA})_3phen]_2$

Juan-Fen Wang,[†,‡] Da-Hai Zhang,[§] Xin Liu,[‡] Ke-Zhong Wu,[‡] and Jian-Jun Zhang*[,†,‡]

Experimental Center, Hebei Normal University, Shijiazhuang 050016, P. R. China, College of Chemistry & Material Science, Hebei Normal University, Shijiazhuang 050016, P. R. China, and Department of Chemistry, Handan College, Handan 056005, P. R. China

The synthesis and structure determination of the Sm(III) complex with 1,10-phenanthroline (phen) and 5-chloro-2-methoxybenzoate (5-Cl-2-MOBA) are reported. The crystal and molecular structure of the complex, as well as its molecular formula and composition $[Sm(5\text{-Cl-2-MOBA})_3phen]_2$, were determined by single-crystal X-ray diffraction, elementary analyses, and infrared (IR) and thermogravimetric/differential thermogravimetric (TG-DTG) measurements. Meanwhile, the molar conductance and the ultraviolet (UV) spectra of the complex were measured and depicted. The crystal of the complex belongs to the triclinic crystal system, space group $p\bar{1}$ with $a = 10.729(2)$ Å, $b = 13.0971(18)$ Å, $c = 13.5925(19)$ Å, $\alpha = 64.376(5)°$, $\beta = 84.571(6)°$, $\gamma = 87.733(7)°$, $V = 1714.3(5)$ Å^3, $Z = 1$, $D_c = 1.719$ t·m^{-3}, $\mu = 2.006$ mm^{-1}, and $F(000) = 882$. Each Sm(III) ion in the crystal is nine-coordinate with a distorted monocapped square antiprismatic comformation. The Sm(III) ion in the complex is coordinated by two O atoms of one chelating bidentate carboxylate group, five O atoms of two bridging bidentate, and two bridging−chelating tridentate carboxylate groups and two N atoms of one 1,10-phenanthroline molecule. The thermal decomposition of $[Sm(5\text{-Cl-2-MOBA})_3phen]_2$ can be divided into three stages. By the Malek method, SB(m,n) was defined as the kinetic model of the first-step thermal decomposition. The activation energy E of this step is 183.63 kJ·mol^{-1}, and the pre-exponential factor ln A is 39.59. The thermodynamic parameters $\Delta G^{\neq}$, $\Delta H^{\neq}$, and $\Delta S^{\neq}$ of activation at the peak temperature were also calculated.

Introduction

A large amount of research has been done on rare earth carboxylate complexes for their fascinating structural properties,[1−9] interesting spectroscopic properties, and potential applications in various areas. They are used as fluorescent probes to study nucleic acids[10,11] in the biological field and preservatives in metal anticorrosion,[12] which has an important significance in our daily life. The various coordination modes of carboxyl groups such as chelating, bridging, and bridging−chelating make the complex structures of rare earth benzoate derivatives more colorful. Lanthanide cations are used as central atoms because they have a higher coordination number and a more flexible coordination geometry than their transition metal analogues.[13] There are binary complexes of rare earth elements with 5-chloro-2-methoxybenzoate obtained as solids, and the focus of the research attention has been on the thermal behavior of the complexes.[14,15] In this paper, we have synthesized the ternary complex of samarium 5-chloro-2-methoxybenzoate with 1,10-phenanthroline, obtained its crystal structure, and discussed its thermal decomposition procedure by thermogravimetric/differential thermogravimetic (TG-DTG) and infrared (IR) techniques. In addition, the corresponding nonisothermal kinetics values were determined from the analysis of the TG-DTG curves of the complex by the Malek method.[16,17]

* Corresponding author. Tel.: +86-31186269386. Fax: +86-31186268405. E-mail address: jjzhang6@126.com.
† Experimental Center, Hebei Normal University.
‡ College of Chemistry & Material Science, Hebei Normal University.
§ Handan College.

Experimental Section

Preparation of the Title Complex. $SmCl_3·6H_2O$ (0.2 mmol) was dissolved in 3 mL of distilled water. 5-Chloro-2-methoxybenzoic acid (5-Cl-2-HMOBA, 0.6 mmol) and 1,10-phenanthroline (phen, 0.2 mmol) were dissolved together in 6 mL of 95 % ethanol solution, adjusting the pH of the solution in a range of 6 to 7 using 1 mol·L^{-1} NaOH solution. Then, the mixture of the two ligands was dropped slowly into the $SmCl_3$ aqueous solution under stirring. The reaction mixture was continually stirred for about 8 h at room temperature and then deposited for 12 h. Subsequently, the precipitate was filtered out, washed three times with 95 % ethanol, and dried in an IR dryer. The powder finally was stored in a silica-gel desiccator for later characterization. The single crystal of the complex was obtained from the mother liquor after two weeks at room temperature. Elemental analyses for $C_{72}H_{52}Cl_6N_4O_{18}Sm_2$: calcd (%): C 48.73, H 2.95, N 3.16, Sm 16.95. Found (%): C 48.87, H 3.04, N 3.13, Sm 17.05.

Chemicals and Apparatus. All chemicals were analytical grade. $SmCl_3·6H_2O$ was prepared by dissolving its oxide in hydrochloric acid and then drying the solution by water-bath heating. The analyses of C, H, and N were carried out with a Vario-EL III elemental analyzer. The metal content was assayed using an ethylenediaminetetraacetic acid disodium salt (EDTA disodium salt) titration method. The IR spectra were recorded on a Bruker TENSOR27 spectrometer using the conventional KBr discs technique at room temperature in the range of (4000 to 400) cm^{-1}. The UV spectra were depicted on a Shimadzu 2501 spectrophotometer. The molar conductance was measured with a Shanghai DDS-307 conductometer. The single crystal

10.1021/je1004565
Published on Web 11/02/2010

Table 1. Important IR Absorption Bands for the Ligands and Complex (cm^{-1})

ligands and complex	$\nu_{C=N}$	ν_{COO}	$\nu_{as(COO^-)}$	$\nu_{s(COO^-)}$	δ_{C-H}		ν_{Sm-O}
phen	1561				854	738	
5-Cl-2-HMOBA		1729					
$[Sm(5\text{-Cl-2-MOBA})_3phen]_2$	1519		1613	1429	844	730	416

X-ray diffraction data were obtained by a Saturn 724+ diffractometer with graphite-monochromated Mo Kα radiation ($\lambda = 0.71073$ A°) at 93(2) K. The structure was solved by direct methods using the SHELXS-97 program[18] and refined by full-matrix least-squares on F^2 using the SHELXL-97 program.[19] TG and DTG experiments for the title complex were conducted using a Perkin-Elmer TGA7 thermogravimetric analyzer under a dynamic N_2 atmosphere in the temperature region of (298.15 to 1173.15) K with a series heating rates of (3, 5, 7, 10, and 15) $K \cdot min^{-1}$ for the study of kinetics.

Results and Discussion

Molar Conductance. The synthesized complex was dissolved in DMSO (dimethylsulfoxide) solution, and its molar conductance was measured with DMSO as a reference. The value is 15.39 $S \cdot cm^2 \cdot mol^{-1}$, indicating that the complex is a nonelectrolyte.[20] The complex is stable at room temperature in air. It is generally soluble in the stronger polar solvents DMSO and dimethylformamide (DMF) and yet insoluble in the usual solvents, such as water, ethanol, and acetone.

IR Spectra. Table 1 illustrates the important IR frequencies of the complex and ligands. The characteristic absorption peaks corresponding to some groups are different between the ligands and the complex. The band at 1729 cm^{-1}, because of the free COOH group in the acid ligand, disappears completely in the spectrum of the complex, whereas two bands at (1613 and 1429) cm^{-1} appear that result from asymmetric and symmetric vibrations of the COO^- group, and the appearance of absorption band at 416 cm^{-1} is attributed to ν_{Sm-O}. These changes indicate that the oxygen atoms from the carboxylate group are coordinated to the Sm^{3+} ion.[21] In addition, $\Delta\nu(COO^-) = 184$ cm^{-1} of the complex is less than that of the sodium salt (209 cm^{-1}), from which we can infer that the acid ligands have a bidentate coordination mode with the Sm^{3+} ion.[22] This result is consistent with the crystal structure of the complex. The bands of $\nu_{C=N}$ (1561 cm^{-1}) and δ_{C-H} [(854 and 738) cm^{-1}] in the spectrum of 1,10-phenanthroline ligand move to low wavenumbers in the spectrum of the complex, suggesting the coordination of the two nitrogen atoms of the neutral ligand to the Sm^{3+} ion.[23]

Ultraviolet (UV) Spectra. The title complex and the two ligands were depicted in DMSO solution by UV spectra with DMSO as a reference. The maximum absorbance λ_{max} of the free ligand 5-Cl-2-HMOBA is 256.10 nm with a molar extinction coefficient of $1.6 \cdot 10^2$ $L \cdot mol^{-1} \cdot cm^{-1}$. The main absorption of the complex $[Sm(5\text{-Cl-2-MOBA})_3phen]_2$ is 264.20 nm, which can be explained by the fact that the free ligands are coordinated to the metal ion, forming a π-conjugated system.[24] Moreover, compared with the complex, the maximum peak of phen at 265.00 nm is similar to that in the complex, suggesting that the formation of the Sm−N bond should have no remarkable influence on the UV absorption of phen.[25] However, the molar extinction coefficient $\varepsilon_{265.00}$ is enhanced from $(3.1 \cdot 10^2$ to $1.02 \cdot 10^3)$ $L \cdot mol^{-1} \cdot cm^{-1}$, suggesting a bigger chelating ring is formed.

Single-Crystal X-ray Diffraction Studies. A single crystal with dimensions of (0.33 × 0.23 × 0.20) mm was selected for measurement. Table 2 gives a summary of the crystallographic data and details of the structural refinements for the title complex. (CCDC 775373 is the number of the Sm(III) complex, which contains the supplementary crystallographic data for this paper. These data can be obtained free of charge from The Cambridge Crystallographic Data Centre via http://www.ccdc.cam.ac.uk/data_request/cif.) The selected bond lengths and angles are listed in Table 3. The molecular structure and the detailed coordination sphere around the Sm(III) ion are shown in Figures 1 and 2.

As shown in Figure 1, two Sm(III) ions, six 5-Cl-2-MOBA groups, and two phen molecules are contained in the molecular structure, which forms a binuclear complex with a crystal-

Table 2. Crystal Data and Structure Refinement for the Title Complex

item	data
empirical formula	$C_{72}H_{52}Cl_6N_4O_{18}Sm_2$
formula weight	1774.58
temperature	93(2) K
wavelength	0.71073 Å
crystal system, space group	triclinic, $p\bar{1}$
unit cell dimensions	$a = 10.729(2)$ Å; $\alpha = 64.376(5)°$ $b = 13.0971(18)$ Å; $\beta = 84.571(6)°$ $c = 13.5925(19)$ Å; $\gamma = 87.733(7)°$
volume	1714.3(5) $Å^3$
Z, calculated density	1, 1.719 $t \cdot m^{-3}$
absorption coefficient	2.006 mm^{-1}
$F(000)$	882
crystal size	(0.33 × 0.23 × 0.20) mm
θ range for data collection	3.02 to 27.50°
limiting indices	$-13 \le h \le 13$, $-16 \le k \le 16$, $-17 \le l \le 17$
reflections collected/unique	17390/7784 [$R_{(int)} = 0.0244$]
completeness to $\theta = 27.50$	98.7 %
absorption correction	semiempirical from equivalents
max. and min. transmission	0.6898 and 0.5547
refinement method	full-matrix least-squares on F^2
data/restraints/parameters	7784/2/474
goodness-of-fit on F^2	1.002
final R indices [$I > 2\sigma(I)$]	$R_1 = 0.0255$, $wR_2 = 0.0572$
R indices (all data)	$R_1 = 0.0293$, $wR_2 = 0.0590$
largest diff. peak and hole	(0.916 and −0.462) $e \cdot Å^{-3}$

Table 3. Selected Bond Lengths (Å) and Angles (deg) for the Title Complex[a]

Bond		Bond	
Sm(1)−O(8)#1	2.3591(16)	Sm(1)−O(4)	2.3794(15)
Sm(1)−O(5)#1	2.3814(16)	Sm(1)−O(7)	2.4630(16)
Sm(1)−O(9)	2.4646(17)	Sm(1)−O(6)	2.4779(16)
Sm(1)−N(1)	2.610(2)	Sm(1)−N(2)	2.643(2)
Sm(1)−O(8)	2.7029(16)		
Angle		**Angle**	
O(8)#1−Sm(1)−O(4)	75.41(6)	O(8)#1−Sm(1)−O(5)#1	75.85(6)
O(4)−Sm(1)−O(5)#1	133.62(5)	O(8)#1−Sm(1)−O(7)	148.65(6)
O(4)−Sm(1)−O(7)	131.73(5)	O(5)#1−Sm(1)−O(7)	88.98(5)
O(8)#1−Sm(1)−O(9)	123.57(5)	O(4)−Sm(1)−O(9)	85.41(6)
O(5)#1−Sm(1)−O(9)	81.10(6)	O(7)−Sm(1)−O(9)	79.60(6)
O(8)#1−Sm(1)−O(6)	147.19(6)	O(4)−Sm(1)−O(6)	78.54(5)
O(5)#1−Sm(1)−O(6)	136.93(5)	O(7)−Sm(1)−O(6)	53.23(5)
O(9)−Sm(1)−O(6)	73.11(6)	O(8)#1−Sm(1)−N(1)	83.68(6)
O(4)−Sm(1)−N(1)	74.21(6)	O(5)#1−Sm(1)−N(1)	136.69(6)
O(7)−Sm(1)−N(1)	89.33(6)	O(9)−Sm(1)−N(1)	140.75(6)
O(6)−Sm(1)−N(1)	70.20(6)	O(8)#1−Sm(1)−N(2)	76.45(6)
O(4)−Sm(1)−N(2)	130.09(6)	O(5)#1−Sm(1)−N(2)	75.76(6)
O(7)−Sm(1)−N(2)	73.25(6)	O(9)−Sm(1)−N(2)	144.31(6)
O(6)−Sm(1)−N(2)	106.69(6)	N(1)−Sm(1)−N(2)	62.39(6)
O(8)#1−Sm(1)−O(8)	73.56(6)	O(4)−Sm(1)−O(8)	68.75(5)
O(5)#1−Sm(1)−O(8)	68.62(5)	O(7)−Sm(1)−O(8)	126.39(5)
O(9)−Sm(1)−O(8)	50.07(5)	O(6)−Sm(1)−O(8)	114.66(5)
N(1)−Sm(1)−O(8)	140.20(5)	N(2)−Sm(1)−O(8)	137.79(5)

[a] Symmetry transformations used to generate equivalent atoms: #1 $-x + 1, -y + 1, -z + 1$.

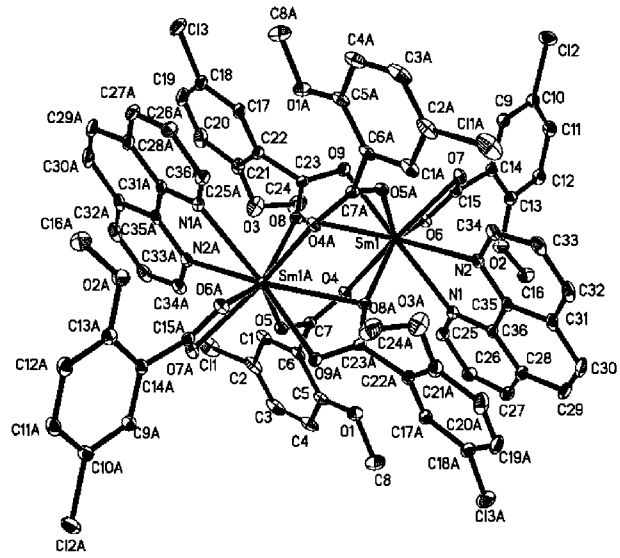

Figure 1. Molecular structure and atom labeling scheme of the complex.

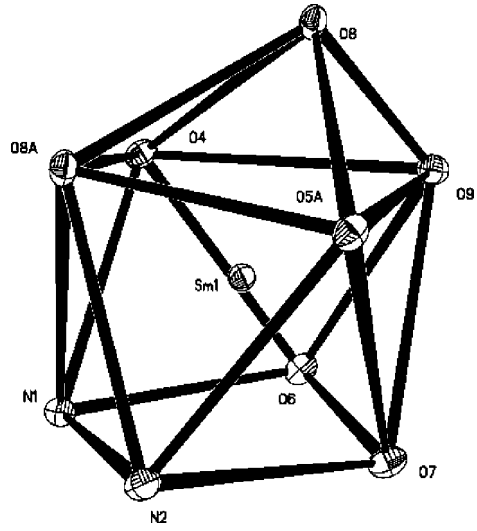

Figure 2. Coordination polyhedron of the Sm(III) ion.

lographic inversion center. In the molecular structure, carboxyl groups have three kinds of coordination modes, chelating bidentate, bridging bidentate, and bridging−chelating tridentate. Each Sm(III) ion is coordinated by seven oxygen atoms from carboxyl groups and two nitrogen atoms from a phen, yielding a distorted monocapped square antiprismatic comformation (Figure 2), in which atom O8 locates at the capped position, atoms O4, O8A, O5A, and O9 form the topside plane of the square antiprism, and the underside plane is formed by atoms N1, N2, O7, and O6. The distances of Sm−O range from [2.3591(16) to 2.7029(16)] Å, and the average distance of Sm−O is 2.4612 Å. Noticeably, the average bond length of Sm−O from the bridging−chelating tridentate carboxylate groups (2.5088 Å) is longer than that of the bridging bidenatte carboxylate groups (2.3804 Å), which can explain the result that part of the carboxyl groups decomposed in the first stage of the thermal decomposition. The length of Sm−N bonds is in the range of [2.610(2) and 2.643(2)] Å with a mean bond length of 2.627(2) Å. By comparing the two bond distances, the bond energy of Sm−O is stronger than the Sm−N bond, so the neutral ligand phen should decompose first, which can be proved well by the thermal decomposition process.

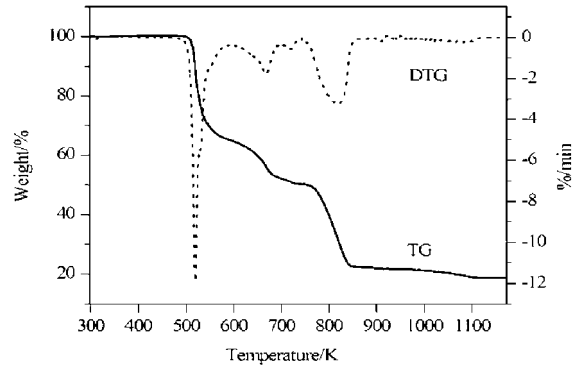

Figure 3. TG-DTG curves of the complex at a heating rate of 7 K·min^{-1}.

Thermal Decomposition Process of the Title Complex. Figure 3 shows the TG-DTG curves of the title complex at a heating rate of 7 K·min^{-1} under a dynamic N_2 atmosphere. As seen from the DTG curve, the thermal decomposition process of the complex presents three stages. The first mass loss is 35.21 % between (473.15 and 591.16) K. It can be easily seen that part of the 5-Cl-2-MOBA ligands have also been decomposed. The IR spectrum of the intermediate residue at 591.16 K shows the disappearance of the absorption band of C═N at 1519 cm^{-1} and the bands of the asymmetric vibrations $\nu_{as(COO^-)}$ at 1613 cm^{-1}, and symmetric vibrations $\nu_{s(COO^-)}$ at 1429 cm^{-1} are weaker than that in the complex, which indicates the two phen (theoretical mass loss is 20.30 %) and part of the 5-Cl-2-MOBA ligands are released together. This is also consistent with the structure analyses. The second and third stages took place at 591.16 K and continued to 1070.8 K with a total loss of 45.19 %, corresponding to the loss of the rest. The characteristic absorptions of the final residue are same as the standard sample spectra of Sm_2O_3. Therefore, up to 1070.8 K, the title complex was completely degraded into Sm_2O_3 with a total loss of 80.40 % (theoretical loss is 80.35 %).

Kinetics of the First Decomposition Stage. The Malek method[16,17] was applied to study the kinetics of the first thermal decomposition process of $[Sm(5\text{-Cl-2-MOBA})_3phen]_2$. As the most important factor for the determination of the function $f(\alpha)$ in the Malek method, the activation energy E of the first decomposition step was calculated by the integral isoconversional nonlinear method (NL-INT method)[26] in the condition of not involving the kinetic function, and the results are listed in Table 4. The average value of E is 183.63 kJ·mol^{-1}, and its standard deviation is 12.63. The average value of E was used to calculate the defined functions $Y(\alpha)$ and $Z(\alpha)$. The needed experimental data of T, α, and $d\alpha/dt$ are obtained from the TG-DTG curves. Functions $Y(\alpha)$ and $Z(\alpha)$ can be obtained by substitution of the experimental data and activation energy E into the following equations:[16]

$$Y(\alpha) = (d\alpha/dt)e^x \quad (1)$$

$$Z(\alpha) = \Pi(x)(d\alpha/dt)T/\beta \quad (2)$$

where $x = E/RT$ and $\Pi(x) = (x^3 + 18x^2 + 88x + 96)/(x^4 + 20x^3 + 120x^2 + 240x + 120)$, which is the expression of the temperature integral. Figures 4 and 5 show the curves of the dependence of $Y(\alpha)$ and $Z(\alpha)$ on α at different heating rates, respectively. From the profiles of the two figures, it can be seen that both $Y(\alpha)$ and $Z(\alpha)$ have a clear maximum when α is more than zero. $Y(\alpha)$ which has a clear maximum indicates that the

Table 4. Values of *E* for the First Step Decomposition of the Complex Obtained by the NL-INT Method

	temperature/K					*E*
α	3 K·min^{-1}	5 K·min^{-1}	7 K·min^{-1}	10 K·min^{-1}	15 K·min^{-1}	kJ·mol^{-1}
0.025	495.8	500.043	505.998	508.713	512.673	184.25
0.05	500.286	504.759	509.702	512.632	516.864	195.88
0.075	502.481	506.933	511.639	514.728	519.161	196.71
0.10	503.96	508.434	513.118	516.286	520.934	195.82
0.125	505.15	509.636	514.28	517.462	522.19	196.10
0.15	506.117	510.681	515.224	518.375	523.169	197.70
0.175	506.781	511.489	515.942	519.161	523.955	196.98
0.20	507.593	512.142	516.517	519.845	524.673	198.43
0.225	508.151	512.677	517.024	520.454	525.321	197.70
0.25	508.665	513.176	517.475	521.007	525.922	197.05
0.275	509.055	513.596	517.913	521.521	526.489	195.28
0.30	509.462	514.033	518.356	522.009	527.06	193.85
0.325	509.812	514.452	518.791	522.504	527.639	191.73
0.35	510.197	514.883	519.179	523.016	528.237	189.79
0.375	510.491	515.326	519.698	523.552	528.874	186.72
0.40	510.894	515.77	520.231	524.115	529.574	183.52
0.425	511.328	516.284	520.775	524.753	530.265	181.81
0.45	511.822	516.885	521.448	525.498	531.144	178.80
0.475	512.369	517.64	522.219	526.412	532.051	175.78
0.50	513.013	518.399	553.011	527.267	533.148	172.55
0.525	513.669	519.212	523.986	528.288	534.257	169.68
0.55	514.54	520.146	524.987	529.341	535.47	166.97
0.575	515.479	521.17	526.071	530.473	536.662	165.60
0.60	516.536	522.343	527.194	531.435	537.477	167.88
0.625	517.428	523.219	528.354	532.203	538.489	168.51
0.65	518.363	524.282	529.233	533.282	539.871	166.13
0.675	519.709	525.498	530.577	534.67	541.403	165.18
0.70	521.143	526.617	531.6	536.045	542.639	166.58
0.725	522.391	527.852	532.784	537.538	543.483	172.67
0.75	524.12	529.494	534.144	539.451	544.766	169.46
0.775	526.325	531.674	536.108	541.527	546.676	176.11
0.80	529.195	534.307	538.534	544.018	548.89	181.72
0.825	532.417	537.5	541.428	547.025	552.01	187.19
0.85	536.407	542.08	545.041	550.607	555.51	197.81
0.875	540.596	545.195	549.016	554.705	559.284	200.12
						183.63[a]
						12.63[b]

[a] Average value of *E*. [b] Standard deviation.

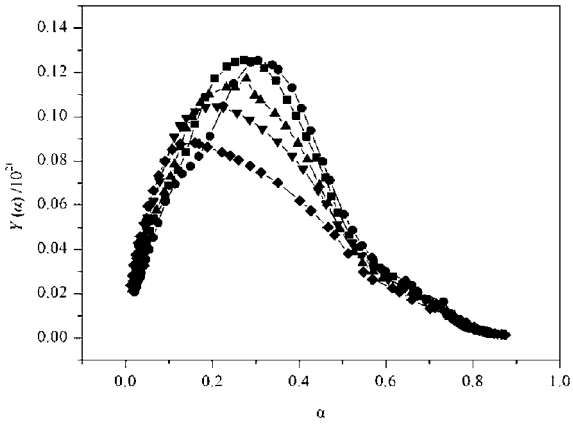

Figure 4. Relationship of $Y(\alpha)$ and α at various heating rates for the first step decomposition: ●, $\beta = 3$ K·min^{-1}; ■, $\beta = 5$ K·min^{-1}; ▲, $\beta = 7$ K·min^{-1}; ▼, $\beta = 10$ K·min^{-1}; ◆, $\beta = 15$ K·min^{-1}.

kinetic model of the first thermal decomposition step of the title complex is JMA($n > 1$) or SM(m,n), while $Z(\alpha)$ has a clear maximum, which is consistent with the fact that the $Z(\alpha)$ function has a maximum at α_p^{∞} for all of the kinetic models summarized in Table 5. To obtain the accurate values of α_m and α_p^{∞}, at which the functions $Y(\alpha)$ and $Z(\alpha)$ have a maximum, the Mathematica 4.1 software was used to fit the curves of $Y(\alpha)-\alpha$ and $Z(\alpha)-\alpha$. It is found that the equations obtained by an eight-time fitting are the most accurate.

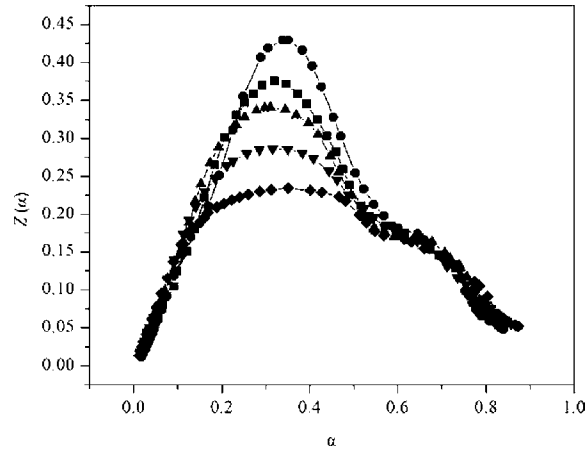

Figure 5. Relationship of $Z(\alpha)$ and α at various heating rates for the first step decomposition: ●, $\beta = 3$ K·min^{-1}; ■, $\beta = 5$ K·min^{-1}; ▲, $\beta = 7$ K·min^{-1}; ▼, $\beta = 10$ K·min^{-1}; ◆, $\beta = 15$ K·min^{-1}.

Table 5. Mathematical Expressions of the Kinetic Models

model	symbol	$f(\alpha)$
Šesták−Berggren equation	SB(m,n)	$\alpha^m(1-\alpha)^n$
Johnson−Mehl−Avrami equation	JMA(n)	$n(1-\alpha)[-\ln(1-\alpha)]^{1-1/n}$
Reaction order equation	RO(n)	$(1-\alpha)^n$
two-dimensional diffusion	D2	$1/[-\ln(1-\alpha)]$
Jander equation	D3	$3(1-\alpha)^{2/3}/2[1-(1-\alpha)^{2/3}]$
Ginstling−Brounshtein equation	D4	$3/2[(1-\alpha)^{-1/3}-1]$

The values of α_m and α_p^{∞} at various heating rates can be obtained by the derivation of the fitted equations listed in Table 6, and Table 7 presents the calculated results. It can be seen from Table 7, $0 < \alpha_m < \alpha_p$ at various heating rates, and the values of α_p^{∞} are not equal to 0.633. In combination with Figure 4 in the literature,[16] the kinetic model of the first thermal decomposition step of the title complex can be determined to be SB(m,n). Furthermore, the kinetic exponents m and n and the pre-exponential factor A were calculated by the following equations:[16]

$$\ln[(d\alpha/dt)e^x] = \ln A + n\ln[\alpha_p(1-\alpha)] \quad (3)$$

$$m = pn \quad (4)$$

$$p = \alpha_m(1-\alpha_m) \quad (5)$$

$$A = -\beta x_p \exp(x_p)/[Tpf'(\alpha p)] \quad (6)$$

where $f'(\alpha_p) = (df(\alpha_p)/d\alpha)$, and the results are given in Table 8.

The thermodynamic parameters of activation can be calculated from the equations:[27,28]

$$A\exp(E/RT) = \nu\exp(-\Delta G^{\neq}/RT) \quad (7)$$

$$\Delta H^{\neq} = E - RT \quad (8)$$

$$\Delta G^{\neq} = \Delta H^{\neq} - T\Delta S^{\neq} \quad (9)$$

where ν is the Einstein vibration frequency, $\Delta G^{\neq}$ the Gibbs energy of activation, $\Delta H^{\neq}$ the enthalpy of activation, and $\Delta S^{\neq}$

Table 6. Fitted Equations for the Curves of $Y(\alpha)-\alpha$ and $Z(\alpha)-\alpha$

$$\beta = 3\ \mathrm{K\cdot min^{-1}}$$
$$Y(\alpha) = -0.11273 + 5.27557\alpha - 64.8954\alpha^2 + 421.572\alpha^3 - 1492.96\alpha^4 + 2994.25\alpha^5 - 3411.5\alpha^6 + 2062.92\alpha^7 - 514.834\alpha^8$$
$$Z(\alpha) = -0.335113 + 13.6033\alpha - 168.738\alpha^2 + 1117.43\alpha^3 - 3925.78\alpha^4 + 7657.4\alpha^5 - 8359.15\alpha^6 + 4777.24\alpha^7 - 1110.77\alpha^8$$

$$\beta = 5\ \mathrm{K\cdot min^{-1}}$$
$$Y(\alpha) = -0.0014094 + 1.34359\alpha - 13.2379\alpha^2 + 101.696\alpha^3 - 417.89\alpha^4 + 902.134\alpha^5 - 1046.86\alpha^6 + 618.823\alpha^7 - 145.776\alpha^8$$
$$Z(\alpha) = -0.0147578 + 1.64826\alpha - 9.13116\alpha^2 + 99.9512\alpha^3 - 402.339\alpha^4 + 597.468\alpha^5 - 142.13\alpha^6 - 393.337\alpha^7 + 251.511\alpha^8$$

$$\beta = 7\ \mathrm{K\cdot min^{-1}}$$
$$Y(\alpha) = 0.0134203 + 0.676211\alpha + 0.390707\alpha^2 - 15.052\alpha^3 + 70.4205\alpha^4 - 207.569\alpha^5 + 359.586\alpha^6 - 317.549\alpha^7 + 109.732\alpha^8$$
$$Z(\alpha) = 0.0170601 + 0.00107423\alpha + 28.5393\alpha^2 - 226.418\alpha^3 + 953.521\alpha^4 - 2451.72\alpha^5 + 3676.63\alpha^6 - 2901.72\alpha^7 + 925.441\alpha^8$$

$$\beta = 10\ \mathrm{K\cdot min^{-1}}$$
$$Y(\alpha) = 0.010668 + 0.897553\alpha + 0.701609\alpha^2 - 39.0866\alpha^3 + 204.671\alpha^4 - 527.332\alpha^5 + 741.939\alpha^6 - 541.432\alpha^7 + 160.062\alpha^8$$
$$Z(\alpha) = 0.0025272 + 0.698345\alpha + 20.9024\alpha^2 - 190.359\alpha^3 + 783.581\alpha^4 - 1836.69\alpha^5 + 2476.07\alpha^6 - 1774.48\alpha^7 + 521.801\alpha^8$$

$$\beta = 15\ \mathrm{K\cdot min^{-1}}$$
$$Y(\alpha) = 0.0822209 + 13.6083\alpha - 75.4887\alpha^2 + 96.1457\alpha^3 + 555.662\alpha^4 - 2569.38\alpha^5 + 4459.19\alpha^6 - 3596.54\alpha^7 + 1119.42\alpha^8$$
$$Z(\alpha) = -0.00111994 + 1.02813\alpha + 18.5549\alpha^2 - 219.244\alpha^3 + 1027.22\alpha^4 - 2549.76\alpha^5 + 3491.71\alpha^6 - 2486.58\alpha^7 + 718.537\alpha^8$$

Table 7. Characteristic Features of the Functions $Y(\alpha)$ and $Z(\alpha)$

β / K·min^{-1}	shape of the curves	α_m	α_p^{∞}	α_p
3	convex	0.3127	0.3373	0.3491
5	convex	0.2800	0.3180	0.3268
7	convex	0.2524	0.3099	0.3105
10	convex	0.2065	0.3096	0.3154
15	convex	0.1572	0.3643	0.3504

Table 8. Kinetic Parameters and the Matched Kinetic Model

β / K·min^{-1}	kinetic model	m	n	ln A	E / kJ·mol^{-1}
3	SB	0.9246	2.0332	40.43	183.63
5	SB	0.6214	1.5979	40.04	
7	SB	0.5934	1.5258	40.02	
10	SB	0.4509	1.7327	39.07	
15	SB	0.3110	1.6674	38.42	
				39.59[a]	

[a] Average value of ln A.

Table 9. Thermodynamic Parameters of the Complex

β / K·min^{-1}	$\Delta G^{\neq}$ / kJ·mol^{-1}	$\Delta H^{\neq}$ / kJ·mol^{-1}	$\Delta S^{\neq}$ / J·mol^{-1}·K^{-1}	T_p / K
3	139.38	179.40	78.43	510.08
5	140.70	179.35	75.14	514.43
7	140.49	179.32	74.91	518.42
10	144.33	179.29	66.95	522.23
15	146.78	179.24	61.45	528.23
average value	142.34	179.32	71.38	

the entropy of activation. The values of these thermodynamic parameters at the peak temperature obtained on the basis of eqs 7 to 9 are summarized in Table 9.

Conclusion

In summary, the title complex has been successfully synthesized, and the crystal structure was determined by single crystal X-ray diffraction. The Sm(III) ion is nine-coordinated with a distorted monocapped square antiprismatic comformation. The thermal decomposition of the complex $[Sm(5\text{-Cl-2-MOBA})_3phen]_2$ occurs in three steps as shown in the text. The kinetic parameters of the first step were determined by the Malek method. The kinetic model is SB(m,n), and the corresponding values of the activation energy E and the pre-exponential factor ln A are 183.63 kJ·mol^{-1} and 39.59. The thermodynamic parameters $\Delta G^{\neq}$, $\Delta H^{\neq}$, and $\Delta S^{\neq}$ of activation at the peak temperature are 142.34 kJ·mol^{-1}, 179.32 kJ·mol^{-1}, and 71.38 J·mol^{-1}·K^{-1}, respectively.

Literature Cited

(1) Lam, A. W. H.; Wong, W. T.; Gao, S.; Wen, G. H.; Zhang, X. X. Synthesis, crystal structure, photophysical and magnetic properties of dimeric and polymeric lanthanide complexes with benzoic acid and its derivatives. *Eur. J. Inorg. Chem.* **2003**, *1*, 149–163.

(2) Qiu, X.; Zhang, Y. B.; Li, X. Synthesis, crystal structure and Fluorescence of a new europium complex with 2-bromobenzoate and 2,2′-bipyridine. *J. Rare Earths* **2009**, *27* (5), 797–800.

(3) Singh, U. P.; Kumar, R.; Upreti, S. Synthesis, structural, photophysical and thermal studies of benzoate bridged Sm(III) complexes. *J. Mol. Struct.* **2007**, *831*, 97–105.

(4) Tian, L.; Ren, N.; Zhang, J. J.; Sun, S. J.; Ye, H. M.; Bai, J. H.; Wang, R. F. Synthesis, Crystal Structure, and Thermal Decomposition Kinetics of the Complex of Dysprosium Benzoate with 2,2′-Bipyridine. *J. Chem. Eng. Data* **2009**, *54*, 69–74.

(5) Ye, H. M.; Ren, N.; Zhang, J. J.; Sun, S. J.; Wang, J. F. Crystal structures, luminescent and thermal properties of a new series of lanthanide complexes with 4-ethylbenzoic acid. *New J. Chem.* **2010**, *34*, 533–540.

(6) Niu, S. Y.; Jin, J.; Jin, X. L.; Yang, Z. Z. Synthesis, Structure and Characterization of Gd(III) Dimer Bridged by Tetra Benzoates. *Solid State Sci.* **2002**, *4*, 1103–1106.

(7) Zhang, J. J.; Zhang, H. Y.; Zhou, X.; Ren, N.; Wang, S. P. Synthesis, Crystal Structure, thermal decomposition kinetics of Sm^{3+} complex with *p*-chlorobenzoic acid and 2,2′-bipyridine. *J. Chem. Eng. Data* **2010**, *55*, 152–158.

(8) Sun, S. J.; Zhang, D. H.; Zhang, J. J.; Ye, H. M.; Wang, S. P.; Wu, K. Z. Crystal structures, luminescent properties and thermal decomposition kinetics of lanthanide complexes with 2-chloro-4-fluorobenzoic acid and 2,20-bipyridine. *J. Mol. Struct.* **2010**, *977*, 17–25.

(9) Ye, H. M.; Ren, N.; Zhang, J. J.; Sun, S. J.; Wang, J. F. Synthesis, crystal structures and thermal decomposition kinetics of four new lanthanide complexes with 3,4-dimethylbenzoic acid and 1,10-phenanthroline. *Struct. Chem.* **2010**, *21* (1), 165–173.

(10) Azab, H. A.; Abd El-Gawad, I. I.; Kamel, R. M. Ternary Complexes Formed by the Fluorescent Probe Eu(III)-Anthracene-9-carboxylic Acid with Pyrimidine and Purine Nucleobases *J. Chem. Eng. Data* **2009**, *54*, 3069–3078.

(11) Topal, M. D.; Fresco, J. R. Fluorescence of terbium ion-nucleic acid complexes: a sensitive specific probe for unpaired residues in nucleic acids. *Biochemistry* **1980**, *19*, 5531–5537.

(12) Blin, F.; Leary, S. G.; Wilson, K.; Deacon, G. B.; Junk, P. C.; Forsyth, M. Corrosion mitigation of mild steel by new rare earth cinnamate compounds. *J. Appl. Electrochem.* **2004**, *34*, 591–599.

(13) Su, Q. *Chemistry of Rare Earths*; Henan Scientific Publications: Henan, China, 1993; p 99 (in Chinese).

(14) Ferenc, W.; Bocian, B. Thermal and Spectral Behaviour of 5-chloro-2-methoxybenzoates of Heavy Lanthanides and Yttrium. *J. Therm. Anal. Calorim.* **2000**, *62*, 831–843.

(15) Czajka, B.; Bocian, B.; Ferenc, W. Investigation of 5-chloro-2-methoxybenzoates La(III), Gd(III) and Lu(III) Complexes. *J. Therm. Anal. Calorim.* **2002**, *67*, 631–642.

(16) Malek, J. The kinetic analysis of non-isothermal data. *Thermochim. Acta* **1992**, *200*, 257–259.

(17) Malek, J.; Smrcka, V. The kinetic analysis of the crystallization processes in glasses. *Thermochim. Acta* **1991**, *186*, 153–169.

(18) Sheldrick, G. M. *SHELXS 97, Program for the Solution of Crystal Structure*; University of Göttingen: Göttingen, Germany, 1997.

(19) Sheldrick, G. M. *SHELXL 97, Program for the Refinement of Crystal Structure*; University of Göttingen: Göttingen, Germany, 1997.

(20) Geary, W. J. The use of conductivity measurements in organic solvents for the characterisation of coordination compounds. *Coord. Chem. Rev.* **1971**, *7*, 81–122.

(21) Shi, Y. Z.; Sun, X. Z.; Jiang, Y. H. *Spectra and Chemical Identification of Organic Compounds*; Science and Technology Press: Nanjing, 1988; p 98 (in Chinese).

(22) Brown, L. M.; Mazadiyasni, K. S. Synthesis and some properties of yttrium and lanthanide isopropoxides. *Inorg. Chem.* **1970**, *9* (12), 2783–2786.

(23) Bai, G. B.; Chen, G. D.; Wang, Z. M.; Yuan, L.; Kang, Z. W.; Gao, J. Z. Synthesis and Characterization of Ln(III)-Glycine-1,10-Phenathroline Ternary Chelates. *Chin. J. Inorg. Chem* **1988**, *4* (2), 32–41; in Chinese.

(24) An, B. L.; Gong, M. L.; Li, M. X.; Zhang, J. M. Synthesis, Structure and Luminescence Properties of Samarium(III) and Dysprosium(III) Complexes with a New Tridentate Organic Ligand. *J. Mol. Struct.* **2004**, *687*, 1–6.

(25) Wang, L. F.; Wu, J. G.; Peng, Z. R.; Ran, W.; Yan, G. H. Study on Ternary Complexes of Rare Earth Elements. IV. Syntheses and Properties of Ternary Complexes of Rare Earth Elements with 3,5-Dinitrosalicylic Acid and Phenanthroline. *Chin. J. Inorg. Chem.* **1990**, *6* (2), 141–146; in Chinese.

(26) Vyazovkin, S.; Dollimore, D. Linear and Nonlinear Procedures in Isoconversional Computations of the Activation Energy of Nonisothermal Reactions in Solids. *J. Chem. Inf. Comput. Sci.* **1996**, *36*, 42–45.

(27) Straszko, J.; Olstak-Humienik, M.; Mozejko, J. Kinetics of Thermal Decomposition of $ZnSO_4 \cdot 7H_2O$. *Thermochim. Acta* **1997**, *292*, 145–150.

(28) Olstak-Humienik, M.; Mozejko, J. Thermodynamic Functions of Activated Complexes Created in Thermal Decomposition Processes of Sulphates. *Thermochim. Acta* **2000**, *344*, 73–79.

Received for review May 2, 2010. Accepted October 15, 2010. This project was supported by the National Natural Science Foundation of China (Nos. 21073053, 21073052, and 20773034), the Natural Science Foundation of Hebei Province (Nos. B2007000237 and E2009000307), and the Education Department Scientific Research Fund from Hebei Province (No. 2008469).

JE1004565